The ion channel of F-ATP synthase is the target of toxic organotin compounds

Christoph von Ballmoos*, Josef Brunner†, and Peter Dimroth*‡

*Institut für Mikrobiologie der Eidgenössischen Technischen Hochschule, ETH Zentrum, CH-8092 Zürich, Switzerland; and †Institut für Biochemie der Eidgenössischen Technischen Hochschule, ETH-Hönggerberg, CH-8093 Zürich, Switzerland

ATP is the universal energy currency of living cells, and the majority of it is synthesized by the F_1F_0 ATP synthase. Inhibitors of this enzyme are therefore potentially detrimental for all life forms. Tributyltin chloride (TBT-Cl) inhibits ATP hydrolysis by the Na^+-translocating ATP synthase of *Ilyobacter tartaricus* or the H^+-translocating counterpart of *Escherichia coli* with apparent K_i of 200 nM. To target the site of this inhibition, we synthesized a tritium-labeled derivative of TBT-Cl in which one of the butyl groups was replaced by a photoactivatable aryldiazirine residue. Upon illumination, subunit a of the ATP synthase becomes specifically modified, and this labeling is suppressed in the presence of the original inhibitor. In case of the Na^+ ATP synthase, labeling is also suppressed in the presence of Na^+ ions, suggesting an interference in Na^+ or TBT-Cl binding to subunit a. This interference is corroborated by the protection of ATP hydrolysis from TBT-Cl inhibition by 105 mM Na^+. TBT-Cl strongly inhibits Na^+ exchange by the reconstituted *I. tartaricus* ATP synthase. Taken together these results indicate that the subunit a ion channel is the target site for ATPase inhibition by toxic organotin compounds. An inhibitor interacting specifically with this site has not been reported previously.

O rganotin compounds are of widespread use in many different areas for >60 years. Tributyltin is broadly used as a preserving agent mainly for wood and textiles and in antifouling paints on ships, leading to severe contamination of aquatic ecosystems. Triphenyltin is applied in agriculture as a pesticide. Dioctyl-, mono-, and dibutyltin serve as stabilizers in plastics (e.g., PVC) and are therefore found in many products of daily use (1, 2).

The general toxicity of organotin compounds is complex and not well understood. In higher organisms, the immune system and production of steroid hormones are affected, e.g., through inhibition of aromatase leading to masculinization (3, 4). Although organotins have been known for decades to act as potent inhibitors of the F_1F_0 ATP synthase (F-ATP synthase), this property has received remarkable little attention and the mechanism of interaction has remained enigmatic (5–7). This lack of knowledge is the more astonishing as the release of an efficient F-ATP synthase inhibitor into the environment may be critical for all life forms. F-ATP synthases play a fundamental role in cellular energy metabolism and are therefore an important constituent of nearly every living cell from bacteria to man.

The ATP synthases are rotary enzymes composed of two motors that are connected by a common shaft to exchange energy with one another (8). During ATP synthesis, the membrane embedded F_0 motor converts energy from an electrochemical transmembrane gradient of protons or Na^+ ions into torque. Rotation is transmitted by the shaft to the water exposed F_1 motor where it drives the synthesis of ATP from ADP and phosphate. Although the structure and function of the F_1 motor is well established (9–11), knowledge of the F_0 motor trails behind (12). An effective approach to gain mechanistic insight into the workings of the F_0 motor is studies with specific inhibitors that target this portion of the F-ATP synthase. A well characterized inhibitor of the F-ATP synthases is dicyclohexyl-carbodiimide (DCCD), which covalently modifies the ion-binding site residues glutamate or aspartate on the c subunits, effectively disabling the F_0 motor from rotation by sterical hindrance. Some 45 years ago, Aldridge (13) described the toxic effect of organotin substances on oxidative phosphorylation in mitochondria. This finding was the beginning of a variety of investigations that showed that all known ATP synthases from bacteria, yeast, and chloroplast to mammalian mitochondria are susceptible to these substances at comparable concentrations. Thereby, tributyltin chloride (TBT-Cl) turned out to be an especially potent inhibitor, although only representing the large variety of organotin compounds, which all act in the same manner (5, 6). TBT-Cl affects the enzyme at levels 10–100 times lower and faster than DCCD. However, as TBT-Cl reacts noncovalently with the enzyme, the site for its interaction is not clear. We reasoned that determination of the binding site could provide important insights into the molecular features of the ATP synthase that are crucial for biological function and at the same time reveal a molecular basis for the toxicology of organotin compounds.

Experimental Procedures

All chemicals were purchased from Fluka or Sigma-Aldrich.

Purification of F-ATP Synthase. The F-ATP synthase was purified from WT *Ilyobacter tartaricus* or *Escherichia coli* cells by fractionated precipitation with polyethyleneglycol (14, 15). The ATP synthase was resuspended in 10 mM Tris·HCl, pH 8.0, and stored in liquid N_2.

Purification of the c_{11} Ring from *I. tartaricus*. The c oligomer of the F-ATP synthase from *I. tartaricus* was purified as described (16).

Determination of ATP-Hydrolyzing Activity. ATP-hydrolyzing activity was determined with the coupled spectrophotometric assay as described (17).

Na^+-Exchange Experiments. The Na^+-exchange measurements were performed as described (18).

Photoaffinity-Labeling Experiments with Photoactivatable Organotin Analog. Incubation mixtures of 100 μl contained 20 μg of purified F-ATP synthase or 10 μg of purified c_{11} from *I. tartaricus* in 50 mM Tris·HCl (pH 8.0)/5 mM $MgCl_2$/0.05% Triton X-100. In competition experiments samples were either incubated with DCCD for 30 min or with Na^+ and organotin derivatives for 60 s before the addition of the tritium-marked photoprobe ([^{3}H]-4-[3-(trifluoromethyl)-3H-diazirin-3-yl]benzyloxymethyl-dibutyl-tin chloride, 1 μM, 1.875 μCi). The mixed sample was then

BIOCHEMISTRY

mounted 10 cm in front of an Hg lamp and immediately (60-s handling time) irradiated for 45 s at $\lambda > 320$ nm and 280 W (350-W Hg lamp, SUSS LH 1,000 lamp house, Waterbury, VT). An unirradiated sample was kept at 4°C as a control.

Workup of Photolabeling Experiments and ^{3}H-Autoradiography/Fluorography. The samples were mixed with SDS to 1% final concentration, subsequently overlaid with 1.2 ml of diisopropyl ether, and shaken by hand for 2 min to remove unbound photolabel from the aqueous solution. The upper organic phase was discarded and the aqueous phase mixed with 5× loading buffer without SDS. An amount of 25 μl (5 μg of protein) was then subjected to SDS/PAGE on a 13.2% gel. The gel was fixed for 30 min (10% acetic acid/30% 2-propanol/60% water) and subsequently incubated for 15 min with enhancer solution (Amersham Pharmacia). The gel was dried in a heat drier system (BioRad) on Whatman paper whereas the other side was covered with water-impermeable foil, which could be removed after drying. Radioactively marked proteins were fluorographically detected by using Hyperfilm MP (Amersham Pharmacia) in a cassette with intensifying screen, which was kept at −80°C for 12–50 h before development. The gels were afterward removed from the Whatman paper and stained with silver.

Chemical Synthesis. *General methods.* TLC was performed on Merck Silica Gel 60F-254 plates. Intermediates and tin-containing substances were detected by fluorescence quenching in UV light (254 nm) or with an organotin reaction spray [(*i*) decomposition of the metallorganic substances by UV light and (*ii*) spray plates with a 0.1% (wt/vol) solution of pyrocatecholviolet in ethanol to stain tin containing bands in bright blue color]. Flash chromatography was performed with Merck 60 (0.04–0.063 mm) silica gel in various solvent mixtures. UV spectra [λ_{max} in nm (log ε)] were recorded in a 1-cm quartz cell. IR spectra were recorded from a 3% CHCl$_3$ solution. ^{1}H NMR (300 MHz) and ^{13}C NMR (75 MHz) were recorded on a Varian Gemini system. Chemical shifts δ are in parts per million (ppm) and coupling constants J in hertz (Hz).

Strategy. The chemical synthesis of the photoactivatable organotin derivative [diazirinedibutyltin chloride (DDBT-Cl)] is depicted in Fig. 1. In brief, we prepared dibutylphenyltin methyl iodide **4** from commercially available dibutyltin dichloride **1** by Grignard reaction, halogenation, and subsequent conversion with Simmons–Smith reagent ICH$_2$ZnI. The methyl iodide **4** was further coupled to a photoactivatable aryldiazirinylmethyl alcohol **5** and the protecting phenyl group was removed by halogenation to obtain the active photolabeling compound **7**. Insertion of a tritium label was obtained by a back-to-back oxidation/reduction reaction of the aryldiazirinylmethyl alcohol **5** with labeled NaB[3H]$_4$ as described for the synthesis of a photoactivatable cholesterol analog (19).

Preparation of Dibutylphenyltin Methyliodide 4. Dibutylphenyltin iodide **3** was prepared by dibutyldiphenyltin **2** from commercially available dibutyltin dichloride **1** as described (20). Synthesis of **4**, which has not been described in the literature, was performed in analogy to the method of Seyferth and Andrews (21). The zinc copper couple was prepared by the method of Le Goff (22). In a 100-ml three-necked, round-bottomed flask, 40 mg of cupric acetate was dissolved in 4 ml of hot acetic acid by using a steam bath. To this solution, 2.6 g of granular zinc was added, and the hot mixture was shaken for 2 min. The solvent was decanted and replaced by 4 ml of acetic acid and the process repeated. The cooled couple was then washed three times with 8 ml of diethyl ether and dried under a stream of nitrogen. The apparatus was completed by a magnetic stir bar, a 50-ml dropping funnel, reflux condenser, and a gas inlet tube. The complete apparatus was dried by heat and strictly kept under nitrogen atmosphere. After
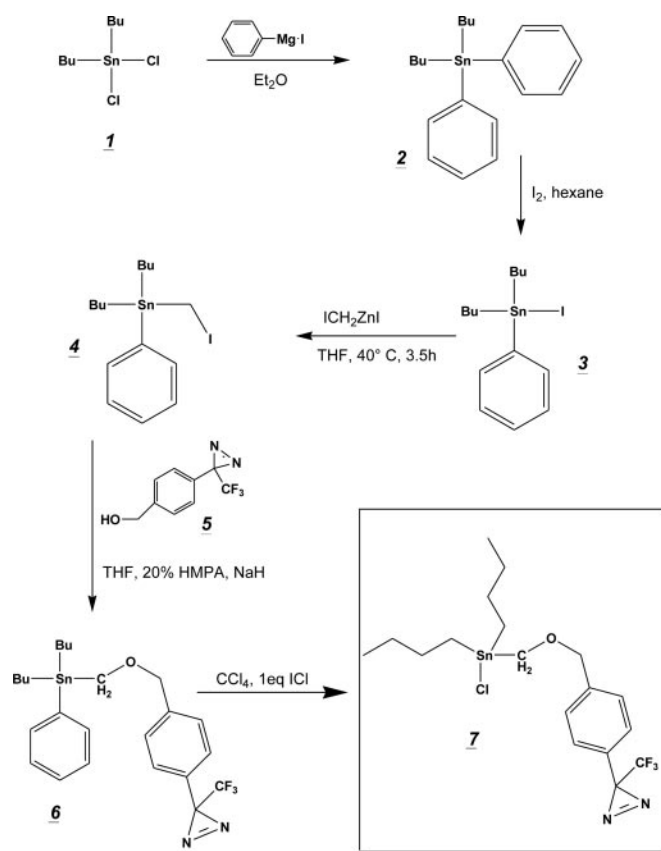

Fig. 1. Chemical synthesis of the photoactivatable organotin derivative **7** (DDBT-Cl). Dibutylphenyltin iodide **3** was prepared as described in the literature by Grignard reaction and subsequent halogenation. Synthesis of **4** was obtained after conversion with Simmons–Smith reagent ICH$_2$ZnI, which was further coupled to an aryldiazirinylmethyl alcohol **5** in the presence of sodium hydride and hexamethylphosphoramide (HMPA). Deprotection of the product **6** was obtained after stoichiometric treatment with iodine monochloride in carbon tetrachloride.

cooling to room temperature, 7 ml of dry tetrahydrofuran (THF) was added to the couple, and the dropping funnel was loaded with 10.2 g of diiodomethane in 7 ml of dry THF. The reaction was started by the addition of a few drops of the diiodomethane solution and slight warming by a heat gun, which could be followed by an exothermic reaction and the formation of a purple color. The reaction mixture was diluted with two volumes of dry THF, and addition of diiodomethane was completed at 40°C. The reaction was allowed to continue for additional 150 min, with mild heating (50°C) during the last hour, by which time most of the couple was consumed.

The mixture was cooled to 0°C and the turbid, grayish suspension was filtered under nitrogen into a dried apparatus similar as described above. The dropping funnel was loaded with 5.6 g (11.5 mmol) of **3** in 12 ml of THF, and the solution was added slowly within 1 h to the mixture kept at 40°C. The reaction was allowed to continue for additional 120 min.

The cooled reaction mixture was treated with 50 ml of benzene and extracted four times each with 40 ml of 5% hydrochloric acid. The organic phase was dried with MgSO$_4$, concentrated, and Kugelrohr-distilled to obtain a colorless liquid (4.5 g, 83%; 90% purity as estimated by TLC). Further purification was performed with flash chromatography by using pure hexane.

The following analytical data were obtained: ^{1}H NMR (CDCl$_3$): 0.9 (t, (CH$_2$)$_3$CH$_3$, 6H); 1.2–1.6 (m, (CH$_2$)$_3$CH$_3$, 12H); 2.18 (t, SnCH$_2$I, 2H); 7.35 (d, J = 8.1, 2H); and 7.47 (m, 3H).

von Ballmoos *et al.*

^{13}C-NMR (CDCl$_3$): 54.15; 127.19; 128.7; 129.38; and 137.5. MS (positive electron impact): found $m/z = 394.9$ (45%) (expected $m/z = 394.9$ for [M-Bu]$^+$); found $m/z = 338.8$ (27%) (expected $m/z = 338.8$ for [M-Bu$_2$]$^+$); and found $m/z = 196.9$ (100%) (expected $m/z = 196.9$ for [M-Bu$_2$PhCH$_2$I]$^+$).

Preparation of 4-[3-(Trifluoromethyl)-3*H***-Diazirin-3-yl]Benzyloxym-ethyl- Dibutylphenyltin 6.** Synthesis of **6** was done as described by Still (23) with the following modifications. Sodium hydride (55–65% dispersion in oil, 50 mg, 1 mmol) was washed three times with pentane and suspended in 7 ml of dry THF in a two-necked, round-bottomed flask. Then 170 mg of diazirine-alcohol **5**, dissolved in 5 ml of THF, was added dropwise to the stirred suspension. After gas evolution had ceased, 384 mg of **4** in 6 ml of THF was added, and the reaction mixture was completed with the addition of 4 ml of hexamethylphosphor-amide. The reaction was stirred for 150 min and then quenched with H$_2$O (10 ml). The mixture was extracted with diethyl ether (3 × 20 ml), and the combined organic phases were washed with brine (20 ml), dried over Na$_2$SO$_4$, and concentrated under reduced pressure. Flash chromatography (hexane/ethyl acetate 20:1) yielded 340 mg (75%) of **6** as colorless oil.

The following analytical data were obtained: ^{1}H NMR (CDCl$_3$): 0.9 (m, (CH$_2$)$_3$CH$_3$, 6H); 1.2–1.6 (m, (CH$_2$)$_3$CH$_3$, 12H); 2.18 (t, SnCH$_2$I, 2H); 7.35 (d, $J = 8.1$, 2H); 7.47 (d, $J = 8.1$, 2H). ^{19}F NMR (CDCl$_3$): −65.0 (s, CF$_3$). ^{13}C NMR (CDCl$_3$): 54.15; 127.19; 128.7; 129.38; and 137.5.

Preparation of 4-[3-(Trifluoromethyl)-3*H***-Diazirin-3-yl]Benzyloxym-ethyl-Dibutyltin Chloride 7.** Halogenation of compound **6** was performed as described (24). A solution of 16.7 mg of ICl in 825 μl of CCl$_4$ was added dropwise to 50 mg of **6** dissolved in 11 ml of CCl$_4$ while stirring at 0°C. After warming up to room temperature (10 min) CCl$_4$ was evaporated under reduced pressure without heating. The slightly purple (iodine) oil was dried under high vacuum for 12 h to remove iodobenzene to yield 38 mg (80%) of **7** as colorless oil. The sample was free from iodobenzene as checked by ^{1}H NMR and was not further purified.

Preparation of [^{3}H]-4-[3-(Trifluoromethyl)-3*H***-Diazirin-3-yl]Benzy-loxymethyl-Dibutyltin Chloride 8.** A solution of **5** (530 mg, 2.31 mmol) in 20 ml of dichloromethane and Dess–Martin periodi-nane (1.3 g, 3.23 mmol, 1.4×) was added at room temperature (25, 26). After stirring for 20 min, the mixture was poured into a mixture of 1 M Na$_2$SO$_3$ (5 ml) and aqueous saturated NaHCO$_3$ (5 ml), and subsequently extracted with dichloromethane (3 × 10 ml). The combined organic solution was concentrated *in vacuo*, and the residual oil was purified by flash chromatography (hexane/ethyl acetate 4:1), and 140 mg (30%) of diazirine aldehyde **8** was obtained as colorless oil. Because the boiling point of the aldehyde is considerably lower than that of the alcohol, most of the material was lost during drying under high vacuum.

To 0.5-ml solution of pure aldehyde **8** (1 mg, 4.6 μmol) in isopropyl alcohol, a solution of 25 mCi of [^{3}H]NaBH$_4$ (0.33 μmol) in 0.1 M NaOH was added, and the mixture was stirred at room temperature for 6 h. Then, 300 μl of 1 M HCl was added, and after 15 min the mixture was extracted with 2 × 1 ml ethyl acetate. The combined organic solution was dried by filtering it through a Pasteur pipette containing MgSO$_4$ and concentrated to a volume of 0.5 ml. The solution was subjected to column chromatography, yielding 11.5 mCi (46%) of ^{3}H-labeled alcohol **5**. The sample was of high purity according to analysis by TLC and autoradiography.
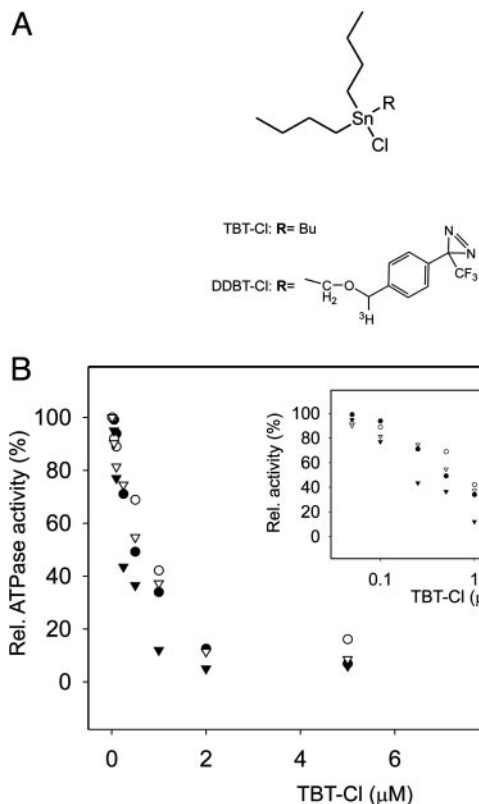

Fig. 2. Chemical structures of TBT-Cl derivatives and inhibition of ATPases. (*A*) Structure of trisubstituted organotin compounds used in this study. TBT-Cl and [^{3}H]DDBT-Cl. (*B*) Inhibition of ATPase by TBT-Cl derivatives. TBT-Cl and detergent-purified ATP synthase from *I. tartaricus* (▲). TBT-Cl and membrane-associated ATP synthase from *I. tartaricus* (●). TBT-Cl and membrane-associated ATP synthase from *E. coli* (○). DDBT-Cl and detergent-purified ATP synthase from *I. tartaricus* (△). (*Inset*) Logarithmic plot.

Results and Discussions

Inhibition Characteristics of Membrane-Bound and Solubilized ATP Synthases. We investigated the effect of TBT-Cl on the Na$^+$-translocating F-ATP synthase of *I. tartaricus* and the H$^+$-translocating ATP synthase from *E. coli* in parallel. Sodium ion translocating F-ATP synthases are close relatives of their proton-translocating counterparts with unique experimental options to explore features of the ion translocation mechanism (12). In the ATP hydrolysis mode, both enzymes displayed a similar response to TBT-Cl, yielding apparent K_i values of 200 nM, comparable with studies with ATPases from other organisms (27) (Fig. 2*B*). Inhibition characteristics were the same for the membrane-bound and detergent-purified enzymes. However, with F$_1$ alone or after disrupting energy coupling with excess detergent (1.5% Triton X-100), the inhibition was abolished, indicating that TBT-Cl affects the F$_0$ part of the enzyme complex.

Synthesis and Application of a Photoactivatable Organotin Derivative (DDBT-Cl). To define the site of TBT-Cl interaction, we chose a photoaffinity-labeling strategy (28). We chemically synthesized a tritium-labeled derivative of TBT-Cl in which one of the butyl groups was replaced by an aryldiazirine residue (Fig. 2*A*; for details see Fig. 1 and *Experimental Procedures*). Upon illumina-tion with UV light, the diazirine is converted into a highly reactive carbene, which forms a covalent photolabeling product with any nearby molecule. The inhibition characteristics of the photoprobe were very similar (Fig. 2*B*) to those of TBT-Cl,
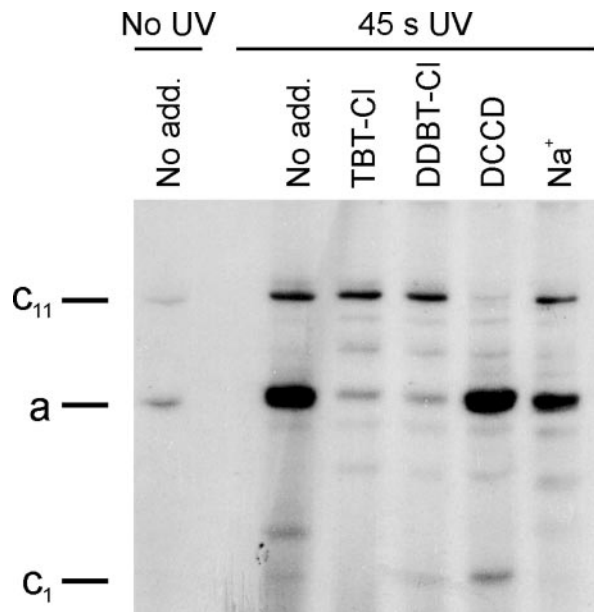
Fig. 3. Photoaffinity-labeling experiments reveal specific interaction of organotins with subunit a. Fluorogram of SDS/PAGE analysis of photoaffinity studies with the ATP synthase from *I. tartaricus*. F-ATP synthase (20 μg, 0.2 mg/ml) in 50 mM Tris·HCl (pH 8.0), 5 mM MgCl$_2$, and 0.05% Triton X-100 was mixed with 1 μM of [^{3}H]DDBT-Cl and irradiated for 45 s with UV light. An unirradiated sample shows that product formation requires photoactivation by UV light. Samples were incubated as indicated with TBT-Cl, DDBT-Cl (50 μM), and NaCl (50 mM) 1 min before addition of the radioactive photolabel, whereas DCCD (50 μM) was added 30 min before the radioactive photolabel.

indicating that the site of interaction with the ATP synthase was the same for both compounds.

Photoaffinity Labeling of ATP Synthase and c-Oligomer with DDBT-Cl. In a typical photolabeling experiment, 20 μg of the purified sodium F-ATP synthase of *I. tartaricus* was mixed with 1 μM radioactive photolabel and illuminated for 45 s with UV light. Analysis of the sample by SDS/PAGE and subsequent fluorography revealed only two radioactive products, which were barely seen in the nonirradiated control (Fig. 3). Clearly, the main product was formed with subunit a, and significantly weaker labeling was found in the oligomeric c ring (c$_{11}$), despite its relative abundance. However, when the sample was pretreated with 50 μM TBT-Cl or the nonradioactive photoprobe, labeling of subunit a was almost completely suppressed, whereas that of c$_{11}$ was not affected. No change in subunit a modification was observed if the sodium-binding sites of the c$_{11}$ ring were partially modified with DCCD. Preincubation of the ATP synthase with 50 mM NaCl showed reduced labeling of subunit a. These data prompted us to perform a more detailed analysis on the interaction of Na$^+$ with the binding of TBT-Cl to subunit a (see below). Photolabeling experiments were repeated with the enzyme reconstituted into lipid bilayers, revealing the same labeling characteristics. Because only modification of subunit a is affected by the addition of competitors, we conclude that the photoprobe specifically binds to subunit a and that the observed weak interaction with subunit c is of a nonspecific nature. Because the diazirine group is ≈ 7 Å apart from the central tin ion, one has to consider the possibility that the organotin-binding site resides on subunits b or c and that the observed labeling of subunit a is due to bridging the distance by the diazirine-containing side chain. Such a scenario, however, is unlikely to cause massive labeling of subunit a side-by-side with no labeling at all of subunit b and only poor unspecific labeling of subunit

c. Furthermore, the ion channel is blocked effectively with low concentrations of TBT-Cl, which does not contain the diazirine compound. Therefore, a site in proximity to the subunit a channel evidently binds DDBT-Cl with high affinity, causing specific autolabeling of this subunit upon irradiation. This conclusion is fully in accord with binding studies performed with the isolated c$_{11}$ ring from *I. tartaricus*. Similar to the binding studies with the enzyme complex described above, the labeling of c subunits of c$_{11}$ was of an unspecific nature, not being competed by the addition of tributyltin chloride or by Na$^+$ ions (data not shown). These findings are in accordance to early photolabeling experiments of the ATP synthase with hydrophobic diazirine compounds in which products were formed preferentially with subunit c (29).

Interaction Studies of TBT with the Na$^+$ Ion-Binding Site on the c-Oligomer. From earlier experiments, subunit c was regarded as the primary target for organotins (6, 30). However, these experiments were unable to exploit the use of a covalent protein-inhibitor complex as reported here. Additional investigations performed at low pH, where the tin chloride bond is broken and a hydrophobic cation is the dominant species in solution (31), indicated that this species binds to the c oligomer and prevents its modification by DCCD. This result is probably due to nonspecific ion pairing of the positive organotin and the negative DCCD-binding amino acid (pK ≈ 7) in the hydrophobic environment of the membrane. Prevention of carbodiimide modification, however, could not be found at pH values > 7 (data not shown).

Influence of Na$^+$ Concentration on Organotin Inhibition. Subunit a harbors the ion channel that provides access to the binding site on the c$_{11}$ ring in the middle of the membrane from the periplasmic surface (28). The channel is essential for the operation of the enzyme, because mutants in which the channel is blocked are completely inactive in both the ATP synthesis and/or coupled ATP hydrolysis mode (32). The channel of subunit a could therefore be the target for the inhibitory organotin compounds. In strong support of this hypothesis is the reduced binding of the photolabel in the presence of Na$^+$ ions as described above (Fig. 3). Further acceptance of this notion is provided by a comparison of ATPase inhibition by TBT-Cl at varying Na$^+$ concentrations. The results of Fig. 4A show a remarkable shift of the apparent K_i of TBT-Cl from 0.2 to 1.5 μM if the Na$^+$ concentration was increased from 5 to 105 mM, indicating competition between TBT-Cl and Na$^+$ for a common binding site on subunit a. The competition between Na$^+$ and TBT-Cl binding was corroborated at a constant inhibitor concentration and varying Na$^+$ concentrations. ATPase inhibition by TBT-Cl decreased from 90 to 30% if the Na$^+$ concentration was raised from 5 to 300 mM. In contrast, no effect was observed with similar concentrations of LiCl or RbCl.

Na$^+$ Transport Studies in Proteoliposomes. A recognition site for Na$^+$ ions in subunit a of the *Propionigenium modestum* (a close relative from *I. tartaricus*) ATP synthase was anticipated from earlier studies when the ion specificity was restricted by mutagenesis to Li$^+$ and H$^+$, and ATP hydrolysis was specifically inhibited by Na$^+$ because of the impaired permeability of the subunit a ion channel for this alkali ion (33). Similar to this mutant phenotype is the inhibition of ATPase activity of the WT enzyme by TBT-Cl, indicating that TBT-Cl could act as a specific blocker of the subunit a ion channel. The results described above on the specific binding of DDBT-Cl to subunit a and the competition between TBT-Cl and Na$^+$ for a common binding site are completely compatible with this supposition. To investigate the effect of TBT-Cl on Na$^+$ translocation directly, we took advantage of a convenient property of the ATP synthase.
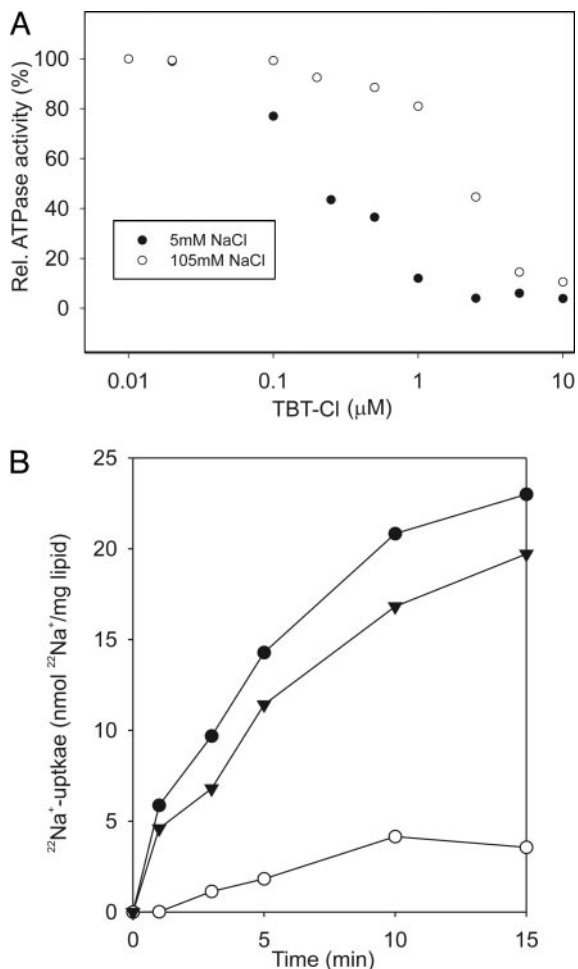
Fig. 4. Evidence for competition between Na^+ and TBT-Cl for binding to the ATP synthase. (*A*) Protection of ATPase from TBT-Cl inhibition by 105 mM NaCl. ATPase activities were determined with the purified enzyme from *I. tartaricus* in the presence of TBT-Cl and NaCl concentrations indicated. (*B*) TBT-Cl blocks the Na^+ channel. $^{22}Na^+/Na^+$-exchange experiments with ATP synthase from *I. tartaricus* reconstituted into liposomes. ●, Control without inhibitor. ▲, ATP synthase preincubated 30 min with 50 μM DCCD. ○, Exchange in presence of 50 μM TBT-Cl.

In absence of an external energy source (membrane potential or ATP), the enzyme rests in an idling mode, which is characterized by back and forth movements of the rotor against the stator within a narrow angle, catalyzing a 1:1 exchange of Na^+ ions between the two reservoirs separated by the membrane (34). This exchange can therefore be followed by the uptake of $^{22}Na^+$ into proteoliposomes, if the radioactive tracer is present at the outside and unlabeled Na^+ is present at the inside. During exchange, every Na^+ traversing the membrane must pass through the subunit a channel. Hence, if the channel is blocked by TBT-Cl, this should abolish $^{22}Na^+$ uptake into the proteoliposomes by $^{22}Na^+_{out}/Na^+_{in}$ exchange. The results of Fig. 4*B* show that this is indeed the case. In control experiments without TBT-Cl, the enzyme catalyzes rapid uptake of $^{22}Na^+$ into the proteoliposomes. This exchange is not significantly affected by modifying part of the binding sites on c_{11} with DCCD in accord with previous measurements (34). In these studies it was shown that modifying part of the rotor sites with DCCD inhibits the rotor sterically from full revolutions but allows back-and-forth movements within a narrow angle, which is sufficient for Na^+ exchange by stator (subunit a) (32) and rotor (c_{11}) channels (15, 16) across the membrane. Prevention of Na^+ exchange by

TBT-Cl treatment indicates direct interference with the ion translocation pathway and is therefore completely compatible with the proposed action of this compound as a blocker of the subunit a ion channel.

Models for Ion Translocation Through the F_0 Part. Two different models have been envisaged for ion translocation through the F_0 motor domain of the Na^+ or H^+ F-ATP synthase, respectively. Sodium ion translocation through the F_0 motor is proposed to proceed by the subunit a channel (inlet channel) from the periplasm to the binding site on the c_{11} rotor ring in the middle of the membrane. After moving the site out of the interface with subunit a by rotation, the ion can diffuse through its intrinsic rotor channel (outlet channel) into the cytoplasmic reservoir, a process that is facilitated by the positive stator charge (R227) at the reentry of the interface (12). Evidence for the inlet channel was obtained by a subunit a triple mutant (33), which specifically abolished Na^+ transport through the channel while retaining transport capacity of Li^+ and H^+, and by the inhibitor studies reported in this communication. Evidence for the intrinsic rotor channels was obtained by demonstrating access of Na^+ or H^+ to the binding sites of the isolated c_{11} ring in solution or in reconstituted liposomes, respectively (15, 16).
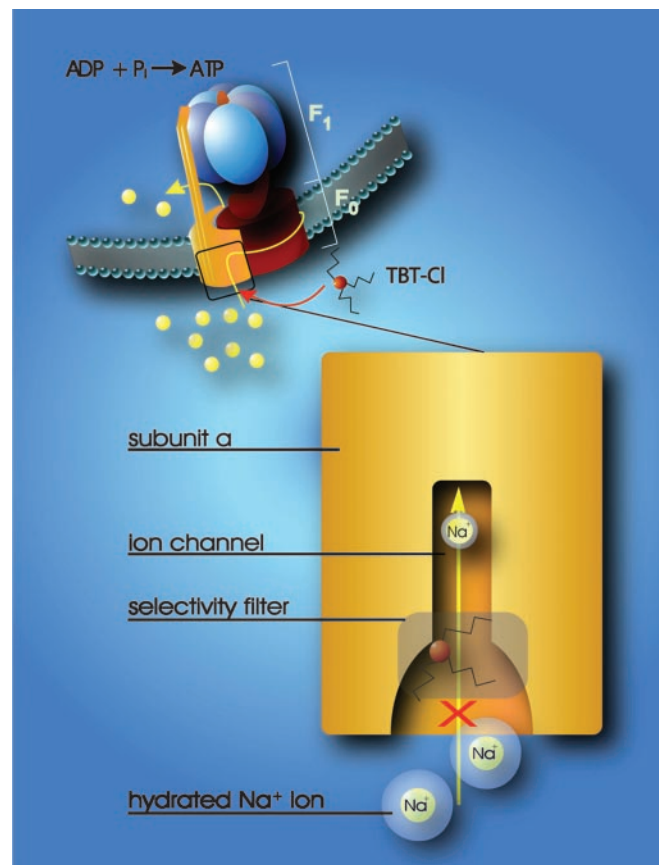

Fig. 5. Model for the interaction of organotin compounds with F-ATP synthases. ATP synthesis from ADP and P_i is coupled to the downhill flux of ions across the membrane-bound F_0 portion. The lower part shows a section through the subunit a channel along the membrane normal. During ATP synthesis hydrated ions enter the mouth of the channel and strip off part of their hydration shell at the selectivity filter (only Na^+ ions can pass the filter). If hydrophobic organotin compounds are present, they accumulate within the membrane and easily penetrate into the entrance of the channel. Here, they interact with a site near the selectivity filter, which disables incoming ions to shed their hydration shell. As a consequence, the ions do not proceed through the channel and ATP synthesis is blocked.

The model for H^+ translocation through the *E. coli* F_0 motor postulates that both the inlet and the outlet channel are located in subunit a and denies any rotor intrinsic channels (35, 36). Hence, both models agree with respect to the inlet channel, and evidence for it has recently been presented by accessibility studies with engineered cysteine residues in subunit a (37). The outlet channel has also been probed by the same technique, but only residues near the cytoplasmic surface could be reached by the aqueous probes. Until now, clear evidence for a cytoplasmic outlet channel on subunit a or on the rotor ring is therefore not available.

Concluding Remarks. Organotin compounds are under intense debate because they were recognized in the 1990s for a variety of disastrous effects in the marine ecosystem. The well known tributyltin, which is used in huge amounts in antifouling paints for large ships, has been called "the most toxic chemical ever deliberately released into the seas" (World Wildlife Fund). Whereas the toxicity toward higher organisms includes a variety of effects, in bacteria, inhibition of the phosphorylation cascade for ATP synthesis seems to be a primary target. Approximately 45 years ago, TBT-Cl was described as a powerful inhibitor for ATP synthases from different organisms, mostly H^+-translocating enzymes of mitochondrial, chloroplast, and bacterial origin (13, 27). This universal inhibitory capacity implies a common structural arrangement conserved among these enzymes. The site of interaction could, however, never be elucidated because of the noncovalent nature of the interaction. Using a photoaffinity-labeling strategy, we could define the site of interaction to be the membrane-embedded a subunit. Subunit a provides a half channel from the periplasmic reservoir to the middle of the membrane through which coupling ions are gated

to reach the binding site on the oligomeric c subunit. We show that in the sodium F-ATP synthase inhibition can be suppressed by high sodium ion concentrations, indicating competition between inhibitor and Na^+ binding.

Summing up, we envisage at the entrance of the subunit a channel a hydrophilic environment, allowing hydrated ions to approach. A recognition site allows the Na^+ ion to shed part of its hydration shell. This process acts as a selectivity filter, similar to the mechanism in the potassium channel, where the size of the hydrated potassium ion is crucial (38). TBT-Cl is proposed to bind near the selectivity filter and to prevent Na^+ ions from passing through the channel. Conversely, Na^+ binding to the recognition site interferes with TBT-Cl binding because the recognition sites for the two compounds are structurally overlapping (Fig. 5). The interaction of organotins on the periplasmic channel in subunit a is compatible with proposed mechanisms for ion translocation in different species despite their discrepancies described above.

This documentation of an ATPase inhibitor that interacts specifically with subunit a has been previously unreported. The periplasmic channel is blocked by TBT-Cl with concomitant inhibition of ATP synthesis or hydrolysis activities. This unique tool will allow directed experiments to unravel details of the ion transport mechanism across the membrane, which may shed light on the mechanism of torque generation by the F_0 motor. The successful application of a photoactivatable organotin analog should be of considerable interest for research toward organotin toxicity in every investigated organism.

1. Fent, K. (1996) *Crit. Rev. Toxicol.* **26,** 1–117.
2. Fent, K. (2003) *Toxicol. Lett.* **140–141,** 353–365.
3. Omura, M., Ogata, R., Kubo, K., Shimasaki, Y., Aou, S., Oshima, Y., Tanaka, A., Hirata, M., Makita, Y. & Inoue, N. (2001) *Toxicol. Sci.* **64,** 224–232.
4. Heidrich, D. D., Steckelbroeck, S. & Klingmuller, D. (2001) *Steroids* **66,** 763–769.
5. Selwyn, M. J. (1976) *Adv. Chem.* **157,** 204–226.
6. Cain, K. & Griffiths, D. E. (1977) *Biochem. J.* **162,** 575–580.
7. Matsuno-Yagi, A. & Hatefi, Y. (1993) *J. Biol. Chem.* **268,** 6168–6173.
8. Boyer, P. D. (1997) *Annu. Rev. Biochem.* **66,** 717–749.
9. Abrahams, J. P., Leslie, A. G., Lutter, R. & Walker, J. E. (1994) *Nature* **370,** 621–628.
10. Capaldi, R. A. & Aggeler, R. (2002) *Trends Biochem. Sci.* **27,** 154–160.
11. Noji, H., Yasuda, R., Yoshida, M. & Kinosita, K., Jr. (1997) *Nature* **386,** 299–302.
12. Dimroth, P., von Ballmoos, C., Meier, T. & Kaim, G. (2003) *Structure (London)* **11,** 1469–1473.
13. Aldridge, W. N. (1958) *Biochem. J.* **69,** 367–376.
14. Neumann, S., Matthey, U., Kaim, G. & Dimroth, P. (1998) *J. Bacteriol.* **180,** 3312–3316.
15. von Ballmoos, C., Meier, T. & Dimroth, P. (2002) *Eur. J. Biochem.* **269,** 5581–5589.
16. Meier, T., Matthey, U., von Ballmoos, C., Vonck, J., Krug von Nidda, T., Kühlbrandt, W. & Dimroth, P. (2003) *J. Mol. Biol.* **325,** 389–397.
17. Laubinger, W. & Dimroth, P. (1988) *Biochemistry* **27,** 7531–7537.
18. Kluge, C. & Dimroth, P. (1992) *Biochemistry* **31,** 12665–12672.
19. Thiele, C., Hannah, M. J., Fahrenholz, F. & Huttner, W. B. (2000) *Nat. Cell Biol.* **2,** 42–49.
20. Marr, I. L., Rosales, D. & Wardell, J. L. (1988) *J. Organomet. Chem.* **349,** 65–74.
21. Seyferth, D. & Andrews, B. S. (1971) *J. Organomet. Chem.* **30,** 151–166.
22. LeGoff, E. (1964) *J. Org. Chem.* **29,** 2048–2050.
23. Still, C. W. (1978) *J. Am. Chem. Soc.* **100,** 1484–1487.
24. Bähr, G. & Pawlenko, S. (1978) *Houben-Weyl Methoden der Organische Chemie* (Thieme, Stuttgart), Vol. 13, pp. 265–288.
25. Weber, T. & Brunner, J. (1995) *J. Am. Chem. Soc.* **117,** 3084–3095.
26. Fang, K., Hashimoto, M., Jockusch, S., Turro, N. J. & Nakanishi, K. (1998) *J. Am. Chem. Soc.* **120,** 8543–8544.
27. Linnett, P. E. & Beechey, R. B. (1979) *Methods Enzymol.* **55,** 472–518.
28. von Ballmoos, C., Appoldt, Y., Brunner, J., Granier, T., Vasella, A. & Dimroth, P. (2002) *J. Biol. Chem.* **277,** 3504–3510.
29. Hoppe, J., Brunner, J. & Jorgensen, B. B. (1984) *Biochemistry* **23,** 5610–5616.
30. Partis, M. D., Griffiths, D. G. & Beechey, R. B. (1984) *Arch. Biochem. Biophys.* **232,** 610–615.
31. Tobias, R. S., Farrer, H. N., Hughes, M. B. & Nevett, B. A. (1966) *Inorg. Chem.* **5,** 2052–2055.
32. Kaim, G. & Dimroth, P. (1998) *Biochemistry* **37,** 4626–4634.
33. Kaim, G., Matthey, U. & Dimroth, P. (1998) *EMBO J.* **17,** 688–695.
34. Kaim, G. & Dimroth, P. (1998) *EMBO J.* **17,** 5887–5895.
35. Vik, S. B. & Antonio, B. J. (1994) *J. Biol. Chem.* **269,** 30364–30369.
36. Junge, W., Lill, H. & Engelbrecht, S. (1997) *Trends Biochem. Sci.* **22,** 420–423.
37. Angevine, C. M., Herold, K. A. & Fillingame, R. H. (2003) *Proc. Natl. Acad. Sci. USA* **100,** 13179–13183.
38. Doyle, D. A., Morais Cabral, J., Pfuetzner, R. A., Kuo, A., Gulbis, J. M., Cohen, S. L., Chait, B. T. & MacKinnon, R. (1998) *Science* **280,** 69–77.